Emulsion Polymerization Reactor Stability: Simplified Model Analysis

A class of simplified emulsion polymerization models is developed. These models include the distribution of particle sizes and radical numbers, and the coupling of the particle initiation rate to the particle size distribution. An analytical solution to the modeling equations is found from contraction mapping. In addition, necessary and sufficient conditions for local stability are derived. These result in a simple criterion for the onset of oscillations in terms of kinetic rate constants and reactor operating conditions. The results clearly show that radical desorption, chain transfer agents, and certain types of impurities should have a strong influence on reactor stability.

J. B. Rawlings, W. H. Ray
Department of Chemical Engineering
University of Wisconsin
Madison, WI 53706

Introduction

Continuous stirred-tank reactors (CSTR) for emulsion polymerization of the type shown in Figure 1 have been known to exhibit isothermal multiple steady states and autonomous oscillations for a wide range of polymers and operating conditions. Indeed the persistence of these unwanted oscillations is one of the obstacles to the acceptance of continuous processes for emulsion polymerization. Table 1 summarizes the pertinent experimental studies displaying sustained oscillations and steady-state multiplicity. Note that oscillations have been reported for the styrene-butadiene, vinyl chloride, styrene, methylmethacrylate, and vinyl acetate systems. The period of these oscillations ranges from three to ten reactor residence times, depending on operating conditions. Styrene and methylmethacrylate polymerizations also are known to exhibit steady-state multiplicity. In this case, two stable monomer conversion branches have been observed as a function of the reactor residence time. What is perhaps most interesting is that all of these phenomena arise under isothermal conditions.

Many investigators have simulated the continuous emulsion polymerization reactor with mathematical models in an attempt to understand these exotic phenomena. After the early steady-state modeling of Gershberg and Longfield (1961), Omi et al. (1969) and Brooks (1973) developed dynamic equations for a few properties of the particle size distribution. The following mechanism was proposed to explain the oscillations:

1. Polymer particles are initiated by radical entry into micelles provided free emulsifier is available (emulsifier concentration is above the critical micelle concentration).

2. The particles polymerize and grow, requiring more free emulsifier to stabilize their increased surface area. Eventually all the free emulsifier is adsorbed on the particles and there are no micelles. Particle initiation then ceases.

3. The large particles eventually wash out of the reactor and micelles reappear due to the emulsifier entering in the feed.

The process then repeats itself indefinitely. The model of Omi et al. has a central inconsistency, however, as pointed out by the authors themselves: A particle area expression, which is only valid at steady state, was used during the entire time integration.

Although they found the model of Omi et al. lacking, Ley and Gerrens (1974) supported the qualitative picture. They experimentally documented each of the mechanistic steps of the oscillation with particle electronmicrographs and surface tension measurements. They introduced the term "generation" to describe all the particles that were formed during a particular period of the oscillation.

More recently, the population balance modeling approach has been used to account for the particle size distribution (PSD). Following the work of Gorber (1973), Dickinson (1976) solved a birth time population balance model to simulate the data of Gerrens et al. (1971) and Ley and Gerrens (1974). Kirillov and Ray (1978) modeled the continuous reactor by adding the inflow and outflow terms to the batch population balance model of Min and Ray (1974). Both steady-state multiplicity and sustained oscillations were simulated. Schork et al. (1980) extended this model to a broader range of polymers.

Kiparissides et al. (1979) also used the birth time population

The current address of J. B. Rawlings is Department of Chemical Engineering, University of Texas, Austin, TX 78712.

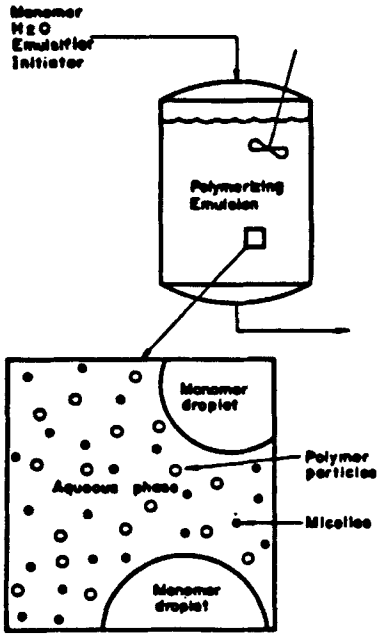

Figure 1. Emulsion polymerization reactor.

balance to model vinyl acetate polymerization. In addition they applied Bendixson's first theorem (Minorsky, 1947, p. 77) to a simplified model's differential equations for total particle number and conversion. Bendixson's first theorem gives a condition under which limit cycles cannot exist in a region. The analysis showed a violation of this condition but does not guarantee the existence of limit cycles. Most recently, Penlidis et al. (1985) also formulated a model using population balance equations.

Chiang and Thompson (1979) studied both the particle age and size population balance equations in order to predict the occurrence of sustained oscillations. After taking the Laplace transform of the particle nucleation function, the stability of the system was found from the Bode stability criterion. However, the conclusions from their stability results are in error, as will be discussed below.

Table 1. Experimental Studies

Investigators	Monomer	Observation
Owen et al. (1947)	Styrene-butadiene	Oscillations
Jacobi (1952)	Vinyl chloride	Oscillations
Gershberg & Longfield (1961)	Styrene	Oscillations
Gerrens et al. (1971)	Styrene	Multiple steady states
Ley & Gerrens (1974)	Styrene	Multiple steady states Oscillations
Greene et al. (1976)	Methylmethacrylate	Oscillations
	Vinyl acetate	Oscillations
Brooks et al. (1978)	Styrene	Oscillations
Kiparissides (1978)	Vinyl acetate	Oscillations
Kiparissides et al. (1980)	Vinyl acetate	Oscillations
Nomura et al. (1980)	Vinyl acetate	Oscillations
Schork et al. (1980)	Methylmethacrylate	Multiple steady states
Schork & Ray (1981)		Multiple steady states
Schork (1981)		Oscillations

Steady-state multiplicity has been attributed to the autoacceleration or gel effect. A maximum of three steady states has been found by including empirical gel effect correlations in the reaction kinetic model (Gerrens et al., 1971; Dickinson, 1976; Kirillov and Ray, 1978; Schork et al., 1980; Rawlings and Ray, 1982, 1986a).

In this paper, we begin with a recently developed, nonlinear comprehensive population balance model (Rawlings and Ray, 1986a). We show that it is possible to make simplifying assumptions that retain the essential features of the model even though quantitative comparisons with data suffer somewhat without the neglected terms. The important point is that this simplified model allows a detailed analytic stability analysis that uncovers the cause of the isothermal oscillation so often observed experimentally. A simple criterion for reactor stability is one of the valuable practical results of the analysis.

Modeling Equations

The comprehensive detailed model of Rawlings and Ray (1986a) has been extensively compared to the CSTR experimental data. These comparisons have shown the model to be capable of simulating all of the interesting reactor dynamics, including oscillations and steady-state multiplicity. The model consists of nonlinear partial differential equations with integral boundary conditions coupled to ordinary differential and algebraic equations. However, detailed insight and general conclusions regarding stability are difficult with such a complex model. Thus we will reduce this rather complex model to one that still retains the essential features, but that is more amenable to analysis.

We start with the population balance in the particles' birth time coordinate. Let $F(t', t)dt'$ represent the concentration of polymer particles at time t having birth times between t' and $t' + dt'$. Assuming no particles in the feed stream and no particle coalescence gives,

$$\frac{\partial(F(t', t)V_R)}{\partial t} = -QF \tag{1}$$

in which Q is the volumetric flow rate from the CSTR and V_R is the reactor volume. Particles are assumed to be initiated by aqueous phase free radicals entering monomer swollen micelles. The birthrate of these particles then gives the boundary condition for the population balance,

$$\text{B.C. } F(t', t) = C_5 V_w R m \quad \text{at } t' = t, t > 0 \tag{2a}$$

in which m is the micelle concentration, R is the aqueous phase radical concentration, V_w is the volume fraction of water in the reactor, and the constants C_i are dimensionless parameters defined in the Notation. For an unseeded reactor, the initial condition is

$$\text{I.C. } F(t', t) = 0 \quad \text{at } -\infty < t' < 0, t = 0 \tag{2b}$$

All of the balances in this work are written in terms of dimensionless variables defined in the Notation.

The coupling of $F(t', t)$ to $m(t)$ through the boundary condition is the central ingredient in the qualitative explanation of the oscillations given above. To extract a simple model retaining this essential feature, we make the following assumptions (three additional assumptions are made subsequently):

1. Constant volume reactor, $V_R = 1$.
2. No density change upon reaction, $d_m = d_p$
3. Constant feed conditions
4. Initial reactor conditions equal to feed conditions
5. Constant aqueous phase radical concentration, $R = R_f$

Assumptions 1–4 are readily understood and are not seriously restrictive, although the constant-density assumption causes noticeable errors when making quantitative comparisons to experimental data (Rawlings and Ray, 1986a). In the full model, the aqueous phase free radical concentration R is nonlinearly coupled to $F(t', t)$ by radical entry into and desorption from particles. As simulations of the full model show, R does vary, but the stability character does not depend on this variation. Thus we may safely assume it to be constant in our anaylsis.

Applying assumptions 1–5 to Eq. 1 and 2 gives,

$$\frac{\partial F(t', t)}{\partial t} = -F \quad -\infty < t' < t, t > 0 \tag{3a}$$

$$\text{B.C. } F(t', t) = k_f m(t') \quad t' = t, t > 0 \tag{3b}$$

$$\text{I.C. } F(t', t) = 0 \quad t' < 0, t = 0 \tag{3c}$$

The solution to Eq. 3 is readily seen to be

$$F(t', t) = k_f m(t') e^{-(t-t')} \quad 0 < t' \le t \tag{4a}$$

$$F(t', t) = 0 \quad t' \le 0 \tag{4b}$$

Specifying m then determines the complete particle distribution at all times. The amount of free emulsifier available to form micelles is taken as the total emulsifier in the reactor less what is required to saturate the aqueous phase and stabilize the particles' surface,

$$m'(t) = C_7(S - S_{wc}) - \frac{C_8}{V_w}\int_{-\infty}^{t} F(t', t) r^2(t', t) dt' \tag{5}$$

Here S is the emulsifier concentration and $r(t', t)$ is the radius of a particle at time t born at time t'. Assumptions 2–4 simplify Eq. 5 to

$$m'(t) = 1 - \frac{C_8}{V_{wf}}\int_{0}^{t} F(t', t) r^2(t', t) dt' \tag{6}$$

If the particles' area becomes large, m' becomes negative, indicating that the aqueous phase is depleted of emulsifier and there are no micelles. The micelle concentration m is therefore given by

$$m = m' H(m') \tag{7}$$

in which H is the Heaviside or unit step function with properties

$$H(m') = \begin{cases} 1 & m' > 0 \\ 0 & m' < 0 \end{cases} \tag{8}$$

Equations 6 and 7 and the boundary condition constitute the on-off particle initiation mechanism. Substituting F into Eq. 6 gives an integral equation for $m'(t)$,

$$m'(t) = 1 - k_f \frac{C_8}{V_{wf}}\int_{0}^{t} m'(t') H(m') e^{-(t-t')} r^2(t', t) dt' \tag{9}$$

Specifying the particle size as a function of birth time completes the model. The particle growth rate is expressed as

$$\frac{\partial r(t', t)}{\partial t} = \left(\frac{1 - C_1}{3} C_6 g_p \frac{\phi}{1 - \phi}\right)\frac{\bar{i}}{r^2} + \frac{r}{3(1 - \phi)}\frac{d\phi}{dt} \tag{10a}$$

$$r(t', t) = 1 \quad t' = t, t > 0 \tag{10b}$$

in which ϕ is the volume fraction of monomer in the particles (assumed independent of r), $\bar{i}$ is the average number of radicals per particle, and g_p is the gel effect for the propagation reaction.

A general relation for $\bar{i}$ was derived by Stockmayer (1957) and O'Toole (1965),

$$\bar{i} = \frac{a}{4}\frac{I_b(a)}{I_{b-1}(a)} \tag{11}$$

in which a and b are given by

$$a = C_{14} r^{(3+n)/2}\sqrt{R/g_t} \tag{12a}$$

$$b = C_{13}\frac{g_{tr}}{g_t}\frac{r^3}{\frac{C_{18}}{\phi} + r^2} \tag{12b}$$

Here n describes the radical entry process. The collision model is defined by $n = 2$ and the diffusion model by $n = 1$.

It is difficult to handle the $\bar{i}$ relation as it stands for several reasons. First, the gel effect for the termination reaction, g_t, is a strongly nonlinear function of ϕ. A low to moderate monomer conversion, ϕ is approximately constant because the reactor contains monomer droplets. The droplets act as a monomer reservoir, saturating the aqueous phase. At high conversion, however, the droplets are consumed, the particles become monomer-starved, and ϕ decreases. To keep the model tractable, we must therefore restrict our attention to operation at conversions where the monomer droplets remain, so that:

Assumption 6.

$$\phi = \phi_{sat}, \text{ constant}$$

This assumption allows us to treat the gel effects as constants as well. Actually, the assumption $\phi = \phi_{sat}$ is found to be a good approximation at conversions well past the droplet disappearance point because the particle monomer concentration drops

rather slowly after the droplets disappear. This is due to the thermodynamic equilibrium with and monomer content of the aqueous phase.

Finally, we must simplify the expression for $\bar{i}$ in order to solve Eq. 10. As an alternative to Eq. 11, consider the familiar power law approximation.

Assumption 7.

$$\bar{i} = k_i r^w \quad 0 \le w < 3 \tag{13}$$

which states that the average number of radicals per particle depends on some power of the particle size, r. The restrictions on w, $0 \le w < 3$, are necessary to have physically realistic particle growth rates. If $w < 0$, larger particles have fewer radicals than smaller particles, which is not a case of physical interest. For $w = 3$, the particle growth rate is exponential, which is unreasonable. If $w > 3$, the particles can reach infinite size in finite time, which is out of the question. The restrictions on w then ensure that the particles have a polynomial growth rate.

We would like to choose w and k_i to approximate the true solution, Eq. 11, in some sense. The power law expression gives a straight-line approximation of $\log(\bar{i})$ vs. $\log(r)$. One is free to establish the criterion by which w and k_i are chosen. One could find the w and k_i that minimize some weighted integral square error between the true and approximate $\bar{i}$ over some range of r values. Another appealing choice is to simply make the approximate $\bar{i}$ solution have the correct large-r dependence. It is easy to show that for large r, Eq. 11 has the asymptote given by

$$\bar{i} = a/4 \tag{14a}$$

$$w = (3 + n)/2 \tag{14b}$$

$$k_i = \frac{C_{14}}{4}(R/g_{to})^{1/2} \tag{14c}$$

Alternatively, one could force the $\bar{i}$ approximation to have the correct small-r dependence. For this case, the power law parameters are

$$w = n \tag{15a}$$

$$k_i = \frac{1}{8}\frac{C_{14}^2 C_{18} R}{C_{13} g_{tr} \phi} \tag{15b}$$

Another case of interest is the classic Smith-Ewart case II kinetics in which $\bar{i} = \frac{1}{2}$ for all particle sizes. For this case the power law parameters are simply

$$\bar{i} = \tfrac{1}{2} \tag{16a}$$

$$w = 0 \tag{16b}$$

$$k_i = \tfrac{1}{2} \tag{16c}$$

It is useful to compare the true solution, Eq. 11, and the particular approximations Eqs. 13–16, for some real experimental systems. Using kinetic and physical parameters for the styrene, methylmethacrylate, and vinyl acetate monomers (Rawlings and Ray, 1986a), we can plot $\bar{i}$ vs. dimensionless particle radius r for the various models. Figures 2–4 show the exact solution,

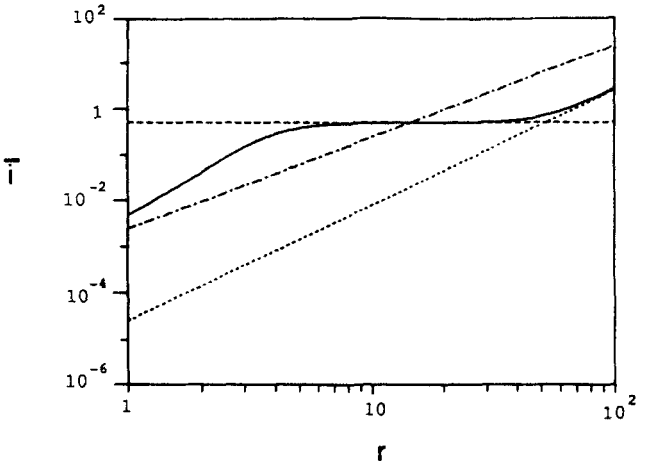

Figure 2. Radical no. vs. particle size for styrene.
$S_f = 0.03$ mol/L; $I_f = 0.03$ mol/L; $V_{wf} = 0.7$, $T = 40$°C.
——— Stockmayer-O'Toole relation, Eq. 11
····· Large-r asymptote, Eq. 14
— — — Small-r asymptote, Eq. 15
----- Smith-Ewart case II, Eq. 16

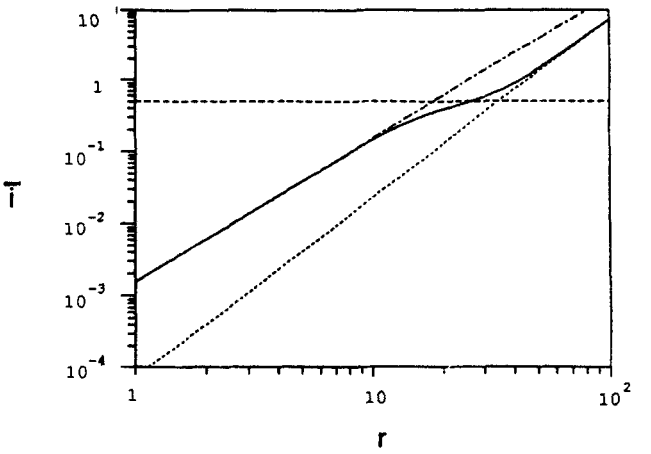

Figure 3. Radical no. vs. particle size for methylmethacrylate.
Data and curve identification as in Figure 2.

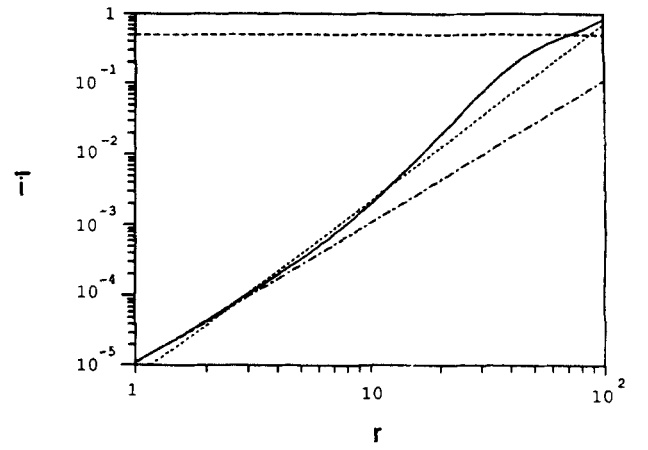

Figure 4. Radical no. vs. particle size for vinyl acetate.
Data and curve identification as in Figure 2.

Eq. 11 (solid line), the large-r asymptote, Eq. 14, the small-r asymptote, Eq. 15, and the Smith-Ewart case II kinetics, Eq. 16. In Figure 2, styrene is not well fitted by any power law approximation. The small-r asymptote is not valid until well below the micelle size, dimensionless radius = 1. The large-r asymptote is not a close approximation until the particle size is very large. In the range of intermediate sizes, Smith-Ewart case II kinetics provides the best fit. For methylmethacrylate, however, Figure 3 shows that the small-r asymptote is a very good approximation out to fairly large sizes. Vinyl acetate, in Figure 4, has the interesting feature that the large-r and small-r asymptotes intersect each other at about $r = 3$. For this case, the large-r asymptote is an excellent approximation to the exact solution over the entire range of particle sizes.

The principal difference between the exact $\bar{i}$ solutions for styrene, methylmethacrylate, and vinyl acetate is the amount of chain transfer to monomer and radical desorption from particles. Figures 2–4 have shown that for each of the three monomers, a power law approximation may be useful in modeling. For a monomer not discussed here, it is a simple task to prepare a plot such those as in Figures 2–4, and determine a power law approximation. One should be careful to note that the exact solution, Eq. 11, is a strong function of the amount of chain transfer agent used, because chain transfer agents induce radical desorption. Thus for operation with a large amount of chain transfer agent, even styrene polymerization could have an $\bar{i}$ relation much like vinyl acetate.

Substituting Eq. 12 into Eq. 9 and solving for r gives,

$$r(t', t) = k_r [(t - t') + v]^{1/(3-w)} \tag{17}$$

where v is an initial condition parameter defined in the Notation. Squaring Eq. 17 for the particle area and substitution into Eq. 9 yields

$$m'(t) = 1 - k_m \int_0^t m'(t')\, H(m') \cdot e^{-(t-t')}\, [(t - t') + v]^{2/(3-w)}\, dt' \tag{18}$$

The solution of Eq. 18 specifies $m'(t)$ and therefore the particle birth time distribution via Eq. 4. Adding the particle size relation, Eq. 17, then specifies the particle size distribution as well.

One other property of interest is the total monomer conversion. The differential equation for total monomer, M, is

$$\frac{dM}{dt} = 1 - M - C_2 C_3 g_{po} \phi_{sat} \int_0^t F(t', t)\, \bar{i}(t', t)\, dt' \tag{19a}$$

$$M(t) = 1 \quad t = 0 \tag{19b}$$

in which the integral accounts for the conversion of monomer to polymer in the particles. Due to the constant density assumption, the conversion is simply $x = 1 - M$.

Solving Eq. 19 and substituting the above relation yields

$$x(t) = k_x \int_0^t m'(t')\, H(m')\, e^{-(t-t')} \cdot [(t - t' + v)^{3/(3-w)} - v^{3/(3-w)}]\, dt' \tag{20}$$

Given m', x is computed from a simple quadrature. The simplified model equations are now complete and are summarized in Table 2.

Model Solution

The micelle equation, Eq. 18, is a nonlinear Volterra integral equation of the second kind. It can be solved numerically by approximating the integral with a quadrature formula, taking steps in t, and solving for $m'(t)$ at each time step. Convergence of the solution is established by decreasing the time step and observing that m' does not change appreciably. A simple computer program was written to calculate m' in this manner using Simpson's rule for the quadrature.

Since the only nonlinearity in the micelle equation appears in the Heaviside function, further analytical progress is possible. One may make the usual assumption that the initial particle size is unimportant due to the large growth rate and make

Assumption 8. $v \approx 0$ so that

$$m'(t) = 1 - k_m \int_0^t m'(t')\, H(m')\, e^{-(t-t')}\, (t - t')^{2/(3-w)}\, dt' \tag{21}$$

It is now possible to piece together an analytical solution. Consider the situation depicted in Figure 5. The reactor starts out at $t = 0$ with $m' = 1$. Particles are generated and m' decreases until $t = t_1$, at which time all the free emulsifier is stabilizing growing particles and particle nucleation ceases. Writing Eq. 21 for this time interval gives

$$m'(t) = 1 - k_m \int_0^t m'(t')\, e^{-(t-t')} \cdot (t - t')^{2/(3-w)}\, dt' \quad 0 < t < t_1 \tag{22}$$

Table 2. Simplified Dynamic Model Equations

$$\bar{i}(t', t) = k_i r^w$$

$$F(t', t) = k_f m'(t') H(m') e^{-(t-t')}$$

$$r(t', t) = k_r [(t - t') + v]^{1/(3-w)}$$

$$m'(t) = 1 - k_m \int_0^t m'(t') H(m') e^{-(t-t')} (t - t' + v)^{2/(3-w)}\, dt'$$

$$x(t) = k_x \int_0^t m'(t') H(m') e^{-(t-t')} [(t - t' + v)^{3/(3-w)} - v^{3/(3-w)}]\, dt'$$

Values of Constants

$$k_f = C_5 R_f V_{wf}$$

$$k_r = \left[\frac{(3 - w)}{3} C_6 g_{po} \frac{\phi_{sat}}{1 - \phi_{sat}} k_i \right]^{1/(3-w)}$$

$$v = (1/k_r)^{3-w}$$

$$k_m = C_8 k_f k_r^2 / V_{wf}$$

$$k_x = C_2 C_3 g_{po} \phi_{sat} k_f k_i k_r^w \frac{(3 - w)}{3}$$

	Smith-Ewart Case II Kinetics	Asymptotic Approximation to Stockmayer-O'Toole	
		At Large r	At Small r
w	0	$\frac{3 + n}{2}$	n
k_i	$\frac{1}{2}$	$\frac{C_{14}}{4} \sqrt{R_f / g_{io}}$	$\frac{1}{8} \frac{C_{14}^2 C_{18} R}{C_{13} g_{io} \phi}$

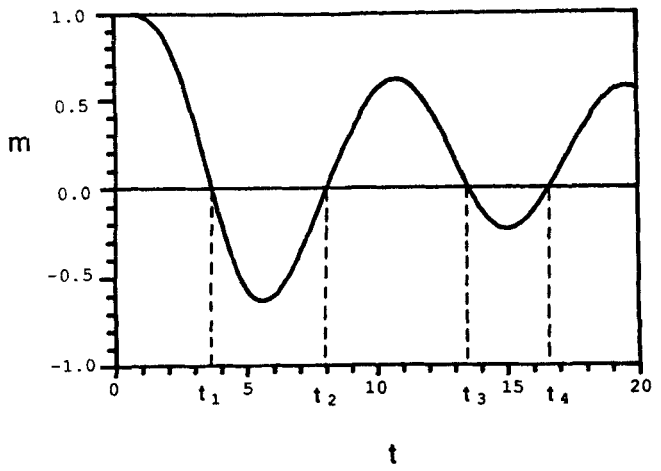

Figure 5. Micelle concentration vs. time.

which is the CSTR analogue of Smith and Ewart's (1984, p. 598) integral equation for the rate of particle formation in the batch reactor.

There are several methods to solve the micelle equations. The first method, employed by Smith and Ewart for batch reactors uses the contraction property of the integral operators. A second method, the use of integral transforms, is discussed later in the stability analysis.

The solution to Eq. 22 using a contraction mapping is now developed. For notational convenience, let

$$c = \frac{5 - w}{3 - w} \tag{23a}$$

$$\alpha = k_m \Gamma(c) \tag{23b}$$

where $\Gamma(c)$ is the complete gamma function.

$$\Gamma(c) \equiv \int_0^\infty t^{c-1} e^{-t}\, dt \tag{24}$$

Rewriting Eq. 22 in the new constants gives

$$m'(t) = 1 - \frac{\alpha}{\Gamma(c)} \int_0^t m'(t') e^{-(t-t')} (t - t')^{c-1}\, dt' \tag{25}$$

We start the contraction to the solution with an initial guess for $m'(t)$,

$$m'_o(t) = 1 \tag{26}$$

Substituting the initial guess into Eq. 25 gives

$$m'_1(t) = 1 - \frac{\alpha}{\Gamma(c)} \int_0^t e^{-(t-t')} (t - t')^{c-1}\, dt' \tag{27}$$

Employing the definition of the incomplete gamma function,

$$\gamma(c, t) = \int_0^t e^{-x} x^{c-1}\, dx = \int_0^t e^{-(t-t')} (t - t')^{c-1}\, dt' \tag{28}$$

we can rewrite Eq. 27 as

$$m'_1(t) = 1 - \frac{\alpha}{\Gamma(c)} \gamma(c, t) \tag{29}$$

Substituting the first iteration into Eq. 25 then gives the second iteration,

$$m'(t) = 1 - \alpha \frac{\gamma(c, t)}{\Gamma(c)} + \frac{\alpha^2}{\Gamma^2(c)} \int_0^t \cdot e^{-(t-t')} (t - t')^{c-1} \gamma(c, t')\, dt' \tag{30}$$

Equation 30 can be simplified with the following formula (Rawlings, 1985, Appendix B),

$$\int_0^t e^{-(t-t')} (t - t')^{a-1} \gamma(b, t')\, dt' = \Gamma(a)\Gamma(b) \frac{\gamma(a + b, t)}{\Gamma(a + b)} \tag{31}$$

Substituting Eq. 31 into Eq. 30 yields,

$$m'_2(t) = 1 - \frac{\alpha \gamma(c, t)}{\Gamma(c)} + \alpha^2 \frac{\gamma(2c, t)}{\Gamma(2c)} \tag{32}$$

Continuing this iteration process leads to

$$m'(t) = \lim_{n \to \infty} m'_n(t) = 1 + \sum_{n=1}^{\infty} (-\alpha)^n \frac{\gamma(nc, t)}{\Gamma(nc)}, \quad 0 \le t \le t_1 \tag{33a}$$

Since Eq. 25 is a linear Volterra equation, the infinite series is guaranteed to converge uniformly to the unique solution (Stakgold, 1979, p. 250). Substituting Eq. 33a into Eq. 20 gives the conversion,

$$x(t) = k_x \Gamma\left(\frac{3c - 1}{2}\right) \sum_{n=0}^{\infty} (-\alpha)^n \frac{\gamma\left(nc + \frac{3c - 1}{2}, t\right)}{\Gamma\left(nc + \frac{3c - 1}{2}\right)} \tag{33b}$$

If the continuous reactor goes to steady state without ever depleting the micelles (α small), then Eq. 33 is the solution for all t. If the micelles are depleted, then we may determine the value of t_1 at which this first occurs from

$$0 = 1 + \sum_{n=1}^{\infty} (-\alpha)^n \frac{\gamma(nc, t_1)}{\Gamma(nc)} \tag{34}$$

Unfortunately, a closed form solution of Eq. 34 for t_1 (α) does not appear tractable. Given t_1, however, m' can be extended to the next time interval, $t_1 \le t \le t_2$, where as seen in Figure 5, there is no particle nucleation [i.e., $H(m') = 0$ in Eq. 21]. Thus over $t_1 \le t \le t_2$

$$m'(t) = 1 - \frac{\alpha}{\Gamma(c)} \int_0^{t_1} m'(t') e^{-(t-t')} (t - t')^{c-1}\, dt' \quad t_1 \le t \le t_2 \tag{35}$$

Since $m'(t')$ is available from Eq. 33, the righthand side can simply be integrated until t_2, at which time the micelles reappear and particle nucleation commences again. In principle, the entire solution could be generated by repeating this process for each of the invervals, $(t_{2_n}, t_{2_{n+2}})$ $n = 0, 1, 2, \ldots$

One has to solve for the t_i numerically, however. Alternatively, one may simply solve the original nonlinear micelle equation numerically, as discussed above.

Finally, the kernel of the nonlinear integral equation can also be shown to satisfy a Lipschitz condition (Stakgold, 1979, p. 249; Davis, 1962, p. 415). This is sufficient to establish the existence and uniqueness of the solution of the nonlinear, simple model, Eq. 18. It is also interesting to note that models similar to Eq. 25 arise in cell population kinetics. Yakovlev et al. (1977) discuss solving these models using Laplace transforms.

Stability Analysis

The stability of the steady states of the simple model is examined next. The steady-state solution of the population balance is

$$F_s(\tau) = k_f m_s e^{-\tau} \quad 0 \leq \tau < \infty \tag{36}$$

in which $\tau = t - t'$ is the particle's age in residence times. From Eq. 18, the steady-state micelle number must satisfy

$$m_s = 1 - k_m m_s \int_0^\infty e^{-\tau}(\tau + v)^{c-1}\, d\tau \tag{37}$$

Solving Eq. 37 yields

$$m_s = \{1 + k_m e^v[\Gamma(c) - \gamma(c, v)]\}^{-1} \tag{38}$$

Assumption 8 (v small) and the definition of α then give the steady-state micelle concentration

$$m_s = \frac{1}{1 + \alpha} \tag{39}$$

The steady state is obviously unique. The absence of steady-state multiplicity is a result of the assumption that ϕ is constant. The strongly nonlinear dependence of the termination rate constant on ϕ is what allows steady-state multiplicity in the detailed model. The influence of the gel effect model on the multiplicity has been recently discussed by Rawlings and Ray (1986a).

The advantage of the simple model is that one does not have to determine the stability of the coupled partial differential equations for F and r. Due to the assumption that the aqueous phase radical concentration R is constant and $\bar{i}$ has the special form, Eq. 13, the partial differential equation for particle size r has a closed form solution. The solution to the particle distribution function F is known once the $m'(t)$ function is determined. Therefore, the stability of the simple model is completely determined by the behavior of $m'(t)$.

Consider a perturbation in the number of micelles, $m_d(t)$.

$$m_d(t) = m'(t) - m_s \tag{40}$$

The steady state, m_s, is defined to be locally asymptotically stable if there exists ϵ such that for all perturbations $|m_d(0)| < \epsilon$, the asymptotic solution is

$$\lim_{t \to \infty} m_d(t) = 0 \tag{41}$$

i.e., the system returns to the steady state after sufficiently small initial perturbations. If ϵ is so large than any bounded initial disturbance will asymptotically approach zero, the steady state is said to be globally asymptotically stable. In the rest of this section, "stable" means stability in the sense of Eq. 41.

We now derive linearized equations describing the time evolution of m_d. Writing Eq. 5 in the particle age description gives

$$m'(t) = C_7(S - S_{wc}) - \frac{C_8}{V_w}\int_0^\infty F(t, \tau)\, r^2(\tau) d\tau \tag{42}$$

Assuming that the reactor has the steady-state particle size distribution at $t = 0$, and subtracting m_s from both sides of Eq. 42, yields

$$m_d(t) = C_7(S - S_{wc}) - 1 - \frac{k_m}{k_r^2}\int_0^t e^{-\tau}\,[m'(t - \tau)\, H(m') - m_s]\, r^2(\tau)\, d\tau \tag{43}$$

Since m_s is positive, linearizing the Heaviside function is trivial,

$$H(m') = H(m_s) + \overbrace{H'(m_s)}^{0}(m' - m_s) = 1 \tag{44}$$

Perturbing the initial value of micelle concentration and substituting the constants listed in Table 2 yields

$$m_d(t) = m_{do}e^{-t} - \frac{\alpha}{\Gamma(c)}\int_0^t m_d(t - \tau)\, e^{-\tau}\tau^{c-1}\, d\tau \tag{45}$$

in which m_{do} is the initial perturbation in the micelle number. The large time solution to this linear Volterra integral equation determines the stability.

One can also solve Eq. 45 as a contraction mapping. This method is not convenient for large t, however, because it results in an infinite sum of increasing powers of t.

Another method to solve the integral equation is to define the integral in Eq. 45 as a state. Repeated differentiation of the new state leads to a set of c autonomous differential equations that are equivalent to Eq. 45. This process works only for c an integer. If c is not an integer, one obtains an infinite number of differential equations, each depending on the next higher one. This is the same problem as obtaining fractional and unclosed moments when using the method of moments.

Because Eq. 45 is linear and contains a convolution integral, the use of integral transforms is suggested. Taking the Laplace transform and solving for the micelle deviation variable, one obtains

$$\bar{m}_d(s) = \frac{m_{do}(s + 1)^{c-1}}{(s + 1)^c + \alpha} \tag{46}$$

where s is the customary complex Laplace transform variable. The asymptotic behavior of $m_d(t)$ can be ascertained from the singularities of $\bar{m}_d(s)$ in the complex s plane. If c is an integer, the analysis is straightforward. The denominator of Eq. 46 can be factored into c simple poles. The asymptotic behavior of $m_d(t)$

is determined by the pole with the largest real part. The complete function $m_d(t)$ can be obtained by a partial fraction expansion (Churchill, 1972, pp. 70–78).

If c is not an integer, the procedure is more complicated. In this case, the denominator of Eq. 46 is not an analytic function. It is in fact multivalued, and one has to make a branch cut in the s plane to make it single-valued (Hildebrand, 1976, pp. 568–571). One can then rigorously obtain $m_d(t)$ by evaluating the Bromwich inversion integral (Hildebrand, 1976, pp. 624–628). The asymptotic behavior of $m_d(t)$ is still determined by the poles of $\overline{m}_d(s)$ with the largest real part. The Bromwich integral is evaluated by Rawlings (1985, Appendix C).

Solving for the zeros of the denominator of $\overline{m}_d(s)$ yields

$$s_o = (-\alpha)^{1/c} - 1, \; 5/3 \le c < \infty \tag{47}$$

Finally, the asymptotic behavior of $m_d(t)$ is given by

$$m_d(t) \to \frac{2m_{do}}{c} e^{t\,Re(s_o)} \cos\left[t\,Im(s_o)\right] \quad Re(s_o) \ge 0 \tag{48a}$$

$$m_d(t) \to 0 \quad Re(s_o) < 0 \tag{48b}$$

From Eq. 48 it is clear that the stability of the steady state depends only on the real part of s_o. The values of s_o are plotted as a function of α and c in Figure 6. The parameter $c = (5 - w)/(3 - w)$ arises from the slope in the $\bar{i}$ relation, while the α parameter depends on the slope and the operating conditions. By reducing the residence time of the reactor, α is reduced, while increasing the residence time causes the value of α to increase. Thus for any choice of w in the $\bar{i}$ relation, Eq. 13, and any set of operating conditions resulting in c and α, the transition from stability to instability is determined from Eq. 47 and Figure 6.

Let us choose $w = 0$ ($c = 5/3$) corresponding to Smith-Ewart case II kinetics. Increasing the value of α causes the roots to move along the $c = 5/3$ line in Figure 6 away from the point $(-1, 0)$. Note that for $c = 5/3$, the two roots move further into the left half-plane as α increases. In other words, there are no operating conditions that make the steady state unstable for Smith-Ewart case II kinetics. In fact for $c \le 2$ ($w \le 1$), the reactor will be stable for all operating conditions.

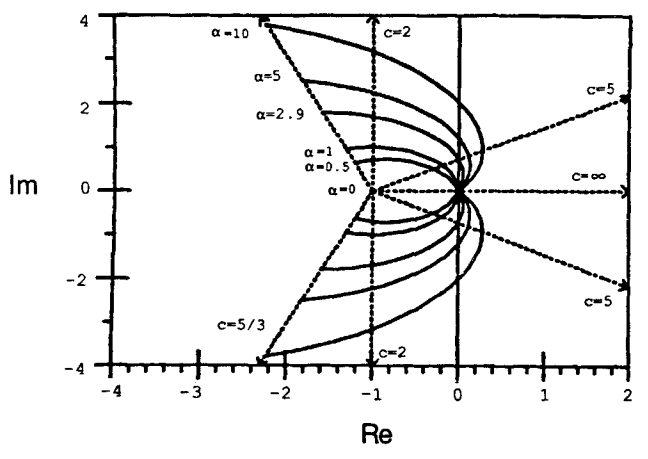

Figure 6. Root locus of linearized micelle equation as a function of c and α.
Smith-Ewart case II kinetics: $c = 5/3$
Asymptote to Stockmayer-O'Toole kinetics: $c = 5$

Consider now the large-r asymptotic Stockmayer-O'Toole kinetics with the collision model ($n = 2$) for radical entry so that $w = 1/2$ ($c = 5$). As α increases from zero, the roots pass into the right half-plane and the steady state becomes unstable. For any value of c, one can solve for the critical value of α at which this transition occurs,

$$\alpha_c = \left[\cos\left(\frac{\pi}{c}\right)\right]^{-c}, \quad 2 < c < \infty \tag{49}$$

For the case of the large-r asymptote to Stockmayer-O'Toole kinetics ($c = 5$), the reactor becomes unstable for $\alpha_c = 2.89$.

Further insight into the effect of the kinetic parameter c on the reactor stability can be gleaned by examining the kernel of Eq. 45

$$k(\tau) = e^{-\tau}\,\tau^{c-1} \tag{50}$$

in which τ is again the dimensionless age of a particle in residence times. The kernel describes how strongly the current m' value is influenced by the past values. The maximum value of k occurs at $\tau = \tau_{max}$, where

$$\tau_{max} = c - 1 \tag{51a}$$

$$k_{max} = e^{-(c-1)}\,(c - 1)^{c-1} \tag{51b}$$

Figure 7 displays k/k_{max} vs. τ for $c = 5/3$, 2, and 5. Note that as c increases, the current state of the reactor is influenced most strongly by states further and further in the past.

Equations such as Eq. 45 were introduced by Volterra in the 1920's to study population dynamics (Scudo, 1971). Using the terminology of this field, kernels with large c denote "strong" delay kernels and those with small c are "weak" delay kernels (Cushing, 1977, p. 6). A physical explanation of the root locus diagram in Figure 6 is that for $c \le 2$, the delay kernel is not strong enough to destabilize the reactor regardless of the operating conditions.

The simple model's stability regions are summarized for all values of α and c in Figure 8. Note that in region I ($c \le 2$), the system is stable for any operating conditions. By maintaining $\alpha < 1$ in region II, the system is stable for any choice of c in the kinetics. For $c > 2$, $\alpha > 1$, the stability is determined by α_c,

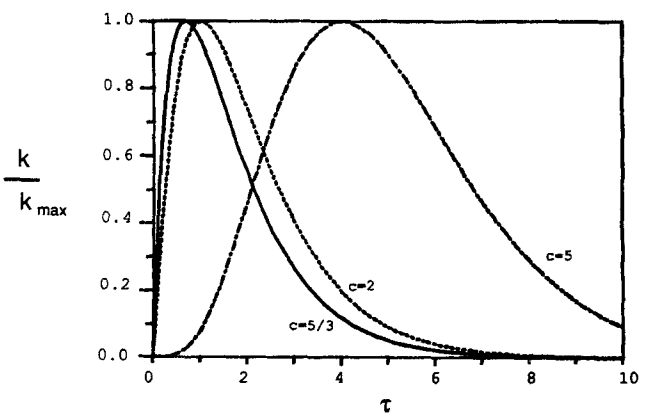

Figure 7. Normalized delay kernal of micelle integral equation.

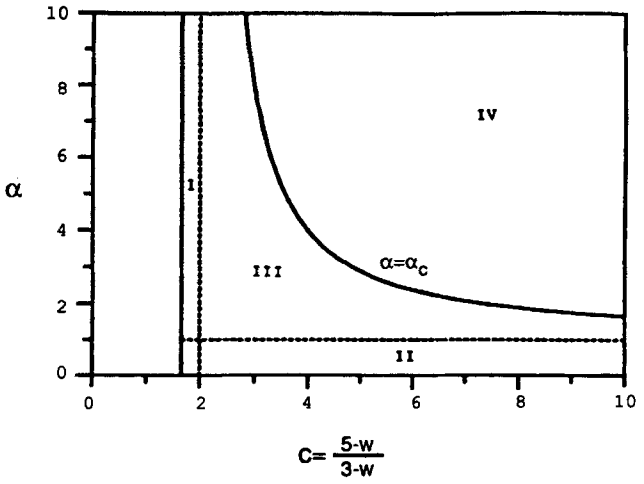

Figure 8. Stability regions for the simple model.
I, stable for all α; II, stable for all c; III, stable; IV, unstable

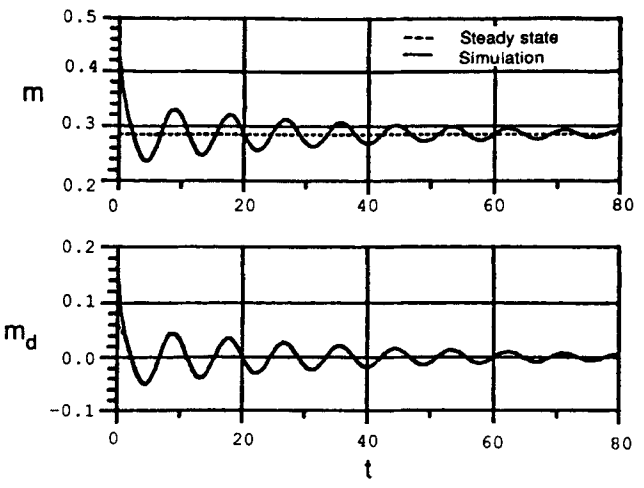

Figure 10. Simulation of micelle equation, stable case.
$c = 5; \alpha = 2.5 < \alpha_c$

which may be calculated from Eq. 49. For $\alpha < \alpha_c$ (region III), the reactor is stable, while for $\alpha > \alpha_c$ (region IV) it is unstable.

One can also solve for the period of the asymptotic solution at the onset of instability, $(\alpha = \alpha_c)$,

$$T = \frac{2\pi}{\tan\left(\frac{\pi}{c}\right)}, \quad c > 2 \tag{52}$$

This result is plotted in Figure 9. Note that the period of the oscillation is longer than eight residence times for the $c = 5$ kinetics, which is in good agreement with the period observed in some experimental studies.

Let us now discuss the character of the instability that arises as α increases beyond α_c. Since the steady state in question is unique and unstable and the solution is bounded, we expect to see some type of periodic behavior for $\alpha > \alpha_c$. Unfortunately, one cannot apply Bendixson's second theorem (Minorsky, 1947, p. 78) to prove the existence of a limit cycle because the system is not described by two autonomous differential equations. However, we may study the nonlinear behavior through numerical simulation.

Let us again consider the large-r asymptotic Stockmayer-O'Toole case ($c = 5$), which as we see in Figures 3 and 4 is a reasonable approximation to the actual $\bar{i}$ for vinyl acetate polymerization. Equation 49 shows that the critical value of α is about $\alpha_c = 2.89$. Figure 10 shows the solution to Eq. 45 for a stable steady state with $\alpha = 2.5$. The initial perturbation, m_{do}, of 0.5 m_s clearly damps away to the steady state.

At the critical value of α, the solution approaches a constant-amplitude oscillation with a period given by Eq. 52. The amplitude of the oscillation is completely determined by the size of the initial perturbation, m_{do}. Figure 11 shows simulations at $\alpha = \alpha_c$ for several different initial perturbations. The steady state for the linearized model at $\alpha = \alpha_c$ is known as a center (Jordan and Smith, 1977). The nonlinear model exhibits the same behavior as the linearized model in the vicinity of the steady state, however. The only difference between the two is the Heaviside function, which does not have an impact until the micelles disappear.

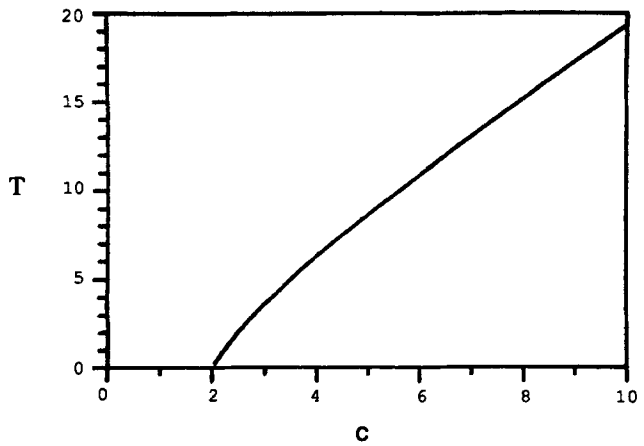

Figure 9. Period of oscillation (residence times) at transition to instability, $\alpha = \alpha_c$, as a function of parameter c.

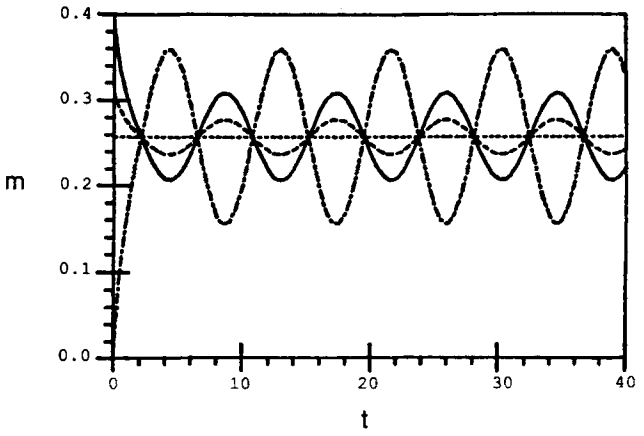

Figure 11. Simulation of micelle equation, transition to instability.
$\alpha = 2.89 = \alpha_c$
——— Steady state
——— $m_{do} = 0.5\ m_s$
– – – $m_{do} = -m_s$
— — $m_{do} = 0.2\ m_s$

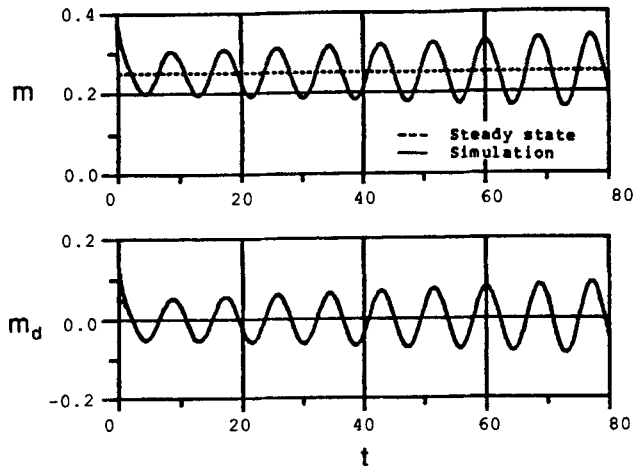

Figure 12. Simulation of micelle equation, unstable case.
$c = 5; \alpha = 3 > \alpha_c$

Therefore, the steady state of the simple nonlinear model is also a center at $\alpha = \alpha_c$.

Finally, the solution to Eq. 45 is plotted for an unstable steady state, $\alpha = 3$. Figure 12 shows that the steady state is indeed unstable for this case and the linearized solution has oscillations with ever-increasing amplitude. However the nonlinear Eq. 43 contains the Heaviside function, which keeps the reactor oscillations bounded in amplitude. In fact, this is one of the most interesting features of the transition to instability. The reactor does not begin oscillating with small amplitude just beyond the transition to instability $\alpha = \alpha_c$, as is usually the case in nonlinear stability problems. Rather, it jumps to a large-amplitude oscillation at $\alpha = \alpha_c$, which is determined by the presence of the Heaviside function at the critical micelle concentration (CMC).

The bifurcation structure for $c = 5$ is summarized in Figure 13. The steady state is unique for all α. The point $\alpha = \alpha_c$ is a center, and the steady state becomes unstable for $\alpha > \alpha_c$. Stable periodic solutions exist for $\alpha > \alpha_c$. Both the maximum and the minimum of the oscillation are plotted as circles in Figure 13a. The period of the stable periodic solutions is plotted in Figure 13b. Figure 13 was prepared by simulating Eq. 18 in time until the period and amplitude of the oscillation did not change significantly.

Numerical calculations indicate that any initial condition is in the region of attraction of the steady state for $\alpha < \alpha_c$. The simple model appears to be globally asymptotically stable in this region. Likewise, any initial condition appears to be in the region of attraction of the stable periodic solution for $\alpha > \alpha_c$. This seems reasonable since there is only one steady state, and it is unstable.

Numerical simulations are presented in Figures 14 to 19 for $c = 5$ and a range of α values. In these simulations the reactor is started up without particles. The operating parameters are:

$$S_f = 0.03 \text{ mol/dm}^3$$

$$I_f = 0.03 \text{ mol/dm}^3$$

$$V_{wf} = 0.70$$

$$T = 40°\text{C}$$

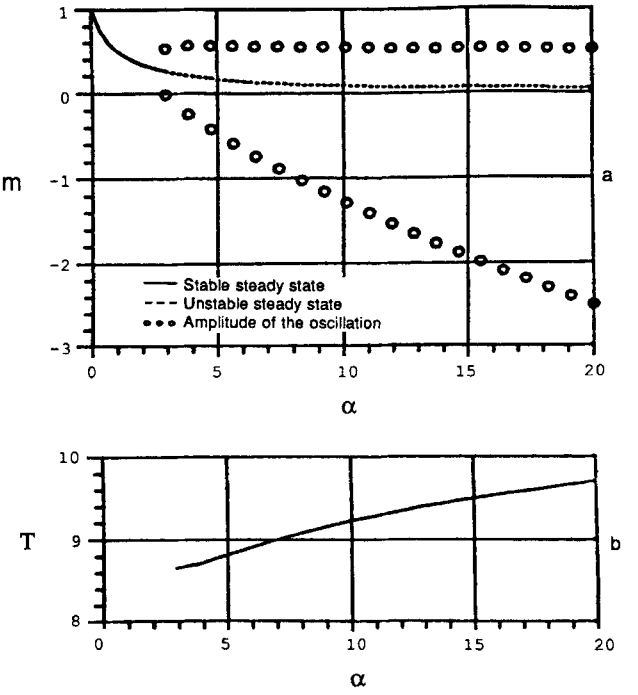

Figure 13. Bifurcation structure of simple model.
a. Steady states and amplitude of oscillation
b. Period of oscillation in residence times
$c = 5; \alpha_c = 2.89$

Parameters given by Rawlings and Ray (1986a) for the polymerization of methylmethacrylate (MMA) are used in the simulations. Sodium dodecyl sulfate is the emulsifier and potassium persulfate is the initiator.

Choosing a residence time of 35 min gives $\alpha = 1.77$, which is stable. Figure 14 shows that the micelle number and conversion both approach the steady state in a damped oscillatory manner. The particle birth time distribution is plotted in Figure 15. Note that after the transients have disappeared, one is able to produce particles with a constant particle size distribution, which is an important factor in obtaining uniform quality product.

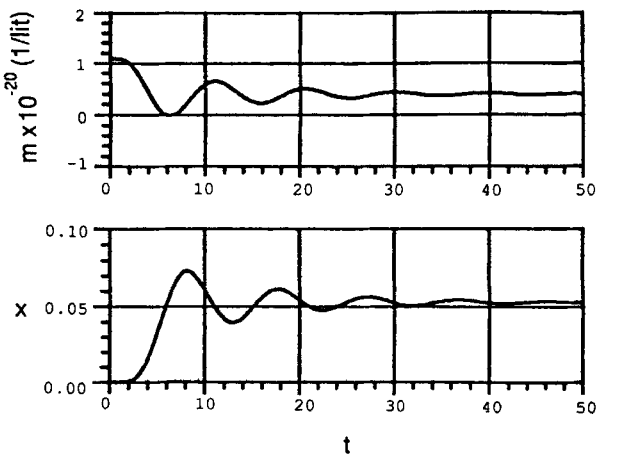

Figure 14. Simulation of simple model; micelles and conversion vs. time for MMA polymerization.
$S_f = 0.03$ mol/L; $I_f = 0.03$ mol/L; $V_{wf} = 0.7$; $T = 40°\text{C}$; $\theta = 35$ min; $\alpha = 1.77 < \alpha_c$ (stable); $c = 5$

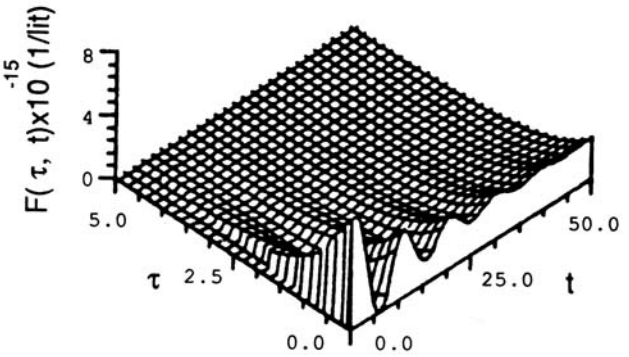

Figure 15. Particle time distribution vs. time for MMA polymerization.
Data as in Figure 14

Contrast the results for a 50 min residence time shown in Figures 16 to 18. For this case, the α value increases to 10.55, so the steady state is unstable. The micelle number and conversion show sustained oscillations with a period of about ten residence times. The conversion oscillation lags about 180 degrees behind the micelle number oscillation. The lag is caused by the time it takes a group of newly formed particles to grow large enough to achieve high reaction rates. The particle time distribution shown in Figure 17 has short periods of rapid particle generation followed by long periods of washout with no particle generation. One cannot obtain a steady particle size distribution under these conditions. A phase plot of reactor conversion vs. micelle number shows the solution winding onto a stable periodic solution. There is no contradiction presented by the curve intersecting itself in the phase plane, since the system is not described by two autonomous differential equations. Increasing the residence time lengthens the period of the oscillation. This is shown in Figure 19 for 70 and 80 min residence times. Further simulations and discussion are provided by Rawlings and Ray (1982) and Rawlings (1985).

For a fixed slope of the $\bar{i}$ vs. r curve (parameters w or c), the parameter α governs the reactor's stability, and it is straightforward to examine the effect of the operating parameters. In order

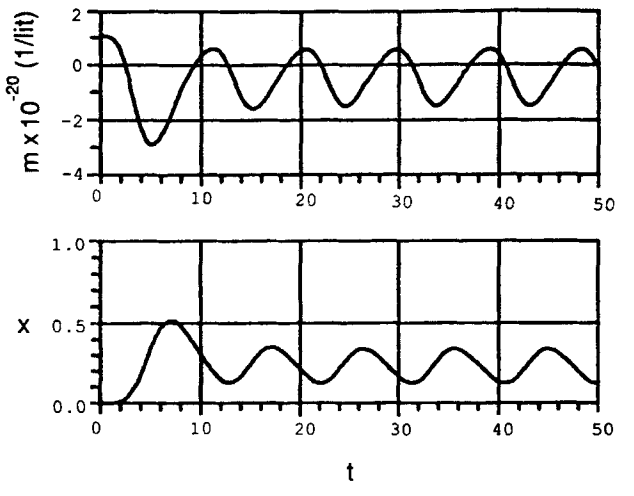

Figure 16. Simulation of simple model; micelles and conversion vs. time for MMA polymerization.
S_f = 0.03 mol/L; I_f = 0.03 mol/L; V_{wf} = 0.7; T = 40°C; θ = 50 min; α = 10.6 > α_c (unstable); c = 5.

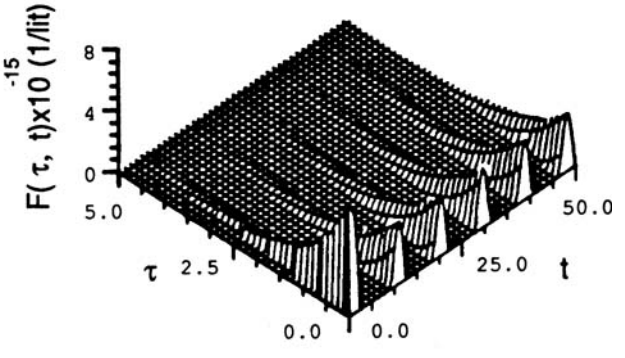

Figure 17. Particle time distribution vs. time for MMA polymerization.
Data as in Figure 16

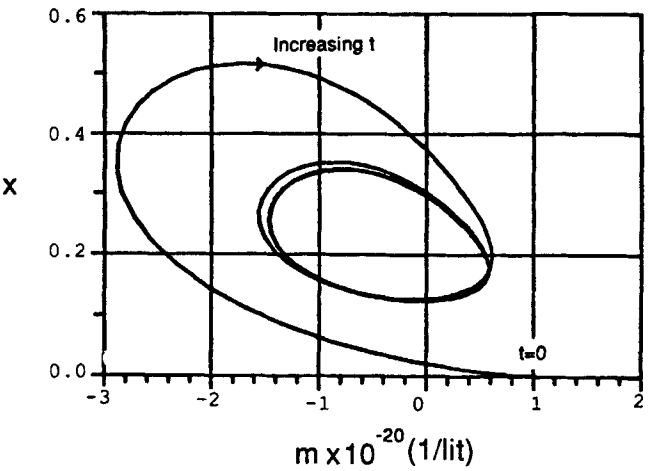

Figure 18. Phase plane projection of conversion vs. micelles for MMA polymerization.
Data as in Figure 16

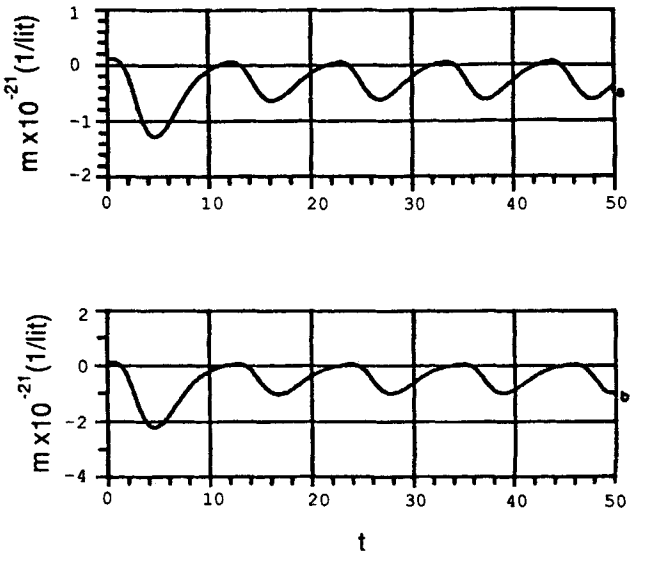

Figure 19. Simulation of simple model; micelles vs. time for MMA polymerization.
a. θ = 70 min, α = 57; b. θ = 80 min, α = 111
c = 5; S_f = 0.03 mol/L; I_f = 0.03 mol/L; V_{wf} = 0.7; T = 40°C

to develop a general expression for α in terms of a chosen slope w and the constants defined in Table 2, one may substitute into the definition of α (Eq. 23b) to yield

$$\alpha = \Gamma\left(\frac{5-w}{3-w}\right)\left(\frac{3-w}{3}\, k_i C_6 g_p \frac{\phi}{1-\phi}\right)^{2/(3-w)} \frac{2fC_4}{C_9}\, C_8 C_5 \quad (53)$$

This can be used to test the stability of the reactor by comparison with α_c.

As special cases, Table 3 lists five possible models arising from the different approximations to the Stockmayer-O'Toole kinetics. Case A is the Smith-Ewart case II kinetics. Cases B and C are the large-r asymptote kinetics with the diffusion and collision models, respectively. Finally, cases D and E are the small-r asymptotic kinetics with the diffusion and collision models. For cases A–E, one substitutes Eqs. 14–16 for k_i and w into Eq. 53 to obtain α for each case:

$$\alpha_A = \left(\frac{1}{2}\right)^{2/3} \Gamma\left(\frac{5}{3}\right)\left(C_6 g_p \frac{\phi}{1-\phi}\right)^{2/3} \frac{2fC_4}{C_9}\, C_8 C_5 \quad (54a)$$

$$\alpha_{B,C} = \Gamma\left(\frac{7-n}{3-n}\right)\left(\frac{3-n}{24}\, C_{14} C_6 \frac{g_p}{\sqrt{g_t}} \frac{\phi}{1-\phi}\right)^{4/(3-n)} \cdot \left(\frac{2fC_4}{C_9}\right)^{(7-n)/(3-n)} C_8 C_5 \quad (54b)$$

$$\alpha_{D,E} = \Gamma\left(\frac{5-n}{3-n}\right)\left(\frac{(3-n)}{24} \frac{C_{14}^2 C_{18}}{C_{13} g_t \phi} C_6 g_p \frac{\phi}{1-\phi}\right)^{2/(3-n)} \cdot \left(\frac{2fC_4}{C_9}\right)^{(5-n)/(3-n)} C_8 C_5 \quad (54c)$$

Choosing $n = 1$ and $n = 2$ (radical entry diffusion and collision models, respectively) in Eq. 54 and substituting the dimensionless constants defined in the Notation gives the general relation for α as

$$\alpha = K\left(\frac{I_f}{S_f - S_{wc}}\right)^p \theta^q \quad (55)$$

The exponents p and q depend on the slope w of the chosen model. Here, the K value for each model depends only on the choice of the physical and kinetic parameters and the temperature. These are listed for styrene, methylmethacrylate, and vinyl acetate monomers in Table 3. Notice that models A and D in the table never predict instability for any operating conditions because $w \leq 1$ ($c \leq 2$). The other models all show that α increases and the reactor tends toward unstable performance for high initiator concentration, high residence time, and low surfactant concentration, although the exact dependence of α on the operating parameters is different for each model.

Table 3. Stability Criteria Parameters for Five Approximate Models

Case, Model	α	w	c	α_c
A. S-E case II	$K_A\left(\frac{I_f}{S_f - S_{wc}}\right)\theta^{5/3}$	0	5/3	∞
B. Large-r diffusion	$K_B\left(\frac{I_f}{S_f - S_{wc}}\right)^2\theta^3$	2	3	8
C. Large-r collision	$K_C\left(\frac{I_f}{S_f - S_{wc}}\right)^3\theta^5$	2.5	5	2.89
D. Small-r diffusion	$K_D\left(\frac{I_f}{S_f - S_{wc}}\right)^2\theta^2$	1	2	∞
E. Small-r collision	$K_E\left(\frac{I_f}{S_f - S_{wc}}\right)^3\theta^3$	2	3	8

Values of K at 40°C, min^{-q}

	Styrene	Methylmethacrylate	Vinyl Acetate
K_A	0.114	0.448	3.66
K_B	4.00×10^{-8}	1.99×10^{-5}	9.87×10^{-5}
K_C	1.14×10^{-13}	2.83×10^{-8}	9.98×10^{-7}
K_D	0.00190	0.00934	0.00154
K_E	3.45×10^{-4}	0.00834	2.27×10^{-4}

Comparison to Other Models and Experimental Data

The simplified model of this paper was derived by applying eight assumptions to the detailed model of Rawlings and Ray (1986a). The major contribution of this paper is the development of analytic conditions for stability using this model. We can now compare these simple stability criteria to the results obtained from a bifurcation analysis of the detailed model. There are of course several limitations of the simplified model that must be taken into consideration in order to make a reasonable comparison. First, the simplified model should not be used if the reactor operation is at high conversion with a monomer that has a significant gel effect. Assumption 6 precludes steady-state multiplicity and a careful treatment of strongly nonlinear gel effects. The full numerical analysis of the detailed model is necessary to handle this operating regime. A second limitation is the applicability of the simple power law approximation of the full Stockmayer-O'Toole $\bar{i}$ relation (assumption 7). Certain monomers, such as styrene in Figure 2, are not well described over the full range of important particle sizes by a simple power law form. We again emphasize that chain transfer agents and impurities can have a big impact on the choice of parameter values in the power law approximation. Figures 3 and 4 show that cases E and C should give a reasonable description for methylmethacrylate and vinyl acetate polymerization, respectively.

We first examine the effect of the eight simplifying assumptions on the stability predictions for methylmethacrylate polymerization. In the bifurcation analysis of the detailed model (described in detail in Rawlings and Ray, 1986a,b), the transition from a stable steady state to a limit cycle occurs when a complex conjugate pair of eigenvalues crosses the imaginary axis into the right half-plane. The computer program that calculates the eigenvalues of the detailed model allows the user to employ any combination of the eight simplifying assumptions used to derive the simplified model. Rawlings (1985) and Rawlings and Ray (1986b) provide a full discussion of the numerical details of this program.

Figures 20 and 21 show the effects of the simplified-model assumptions. The real part of the complex eigenvalue pair with largest real part is plotted vs. residence time in Figure 20. The simplified model (solid line) is in good agreement with the roots

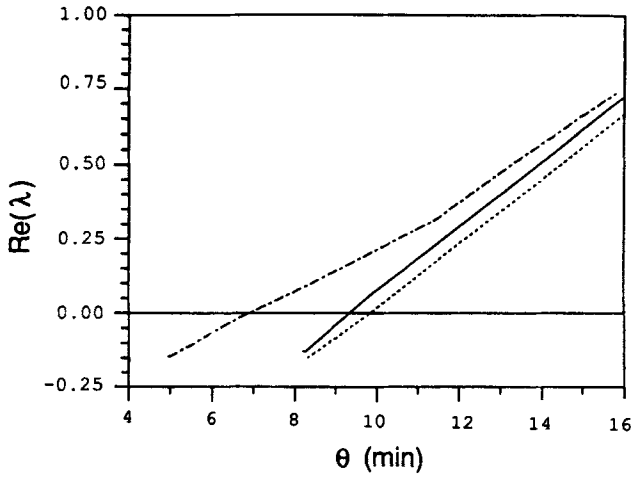

Figure 20. Real part of eigenvalue vs. residence time for MMA polymerization.

S_f = 0.03 mol/L; I_f = 0.03 mol/L; V_{wf} = 0.7; T = 40°C
——— Simplified model, case E, assumptions 1–8
– – – – – Exact $\bar{i}$ relation, assumptions 1–6 and 8
— — — — Full detailed model, no assumptions

of the linearized micelle equation, Eq. 47. The transition to limit cycles occurs at θ = 9.3 min. This can also be found from Table 3 by computing α for case E at these operating conditions. Using the full Stockmayer-O'Toole $\bar{i}$ relation (dotted line) with the other simplified-model assumptions has only a small impact on the eigenvalues, and the transition to instability increases to θ = 10 min. Thus for methylmethacrylate polymerization, case E is a valid approximation to the Stockmayer-O'Toole relation for the stability analysis. Of the other seven assumptions, the biggest changes in the eigenvalues are caused by the constant-density assumption and the constant aqueous phase radical concentration. None of the assumptions changes the essential features of the plot, however. There is always a single residence time at which a pair of eigenvalues crosses into the right half-plane. There is even reasonable quantitative agreement between the detailed and simplified models since some of the assumptions have opposite effects and compensate each other. For example,

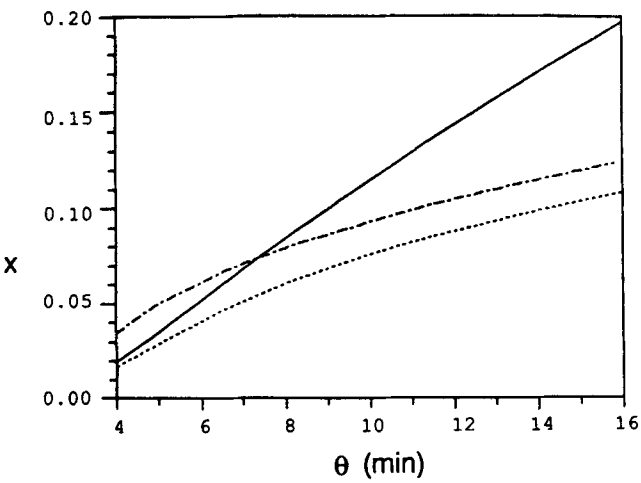

Figure 21. Steady state conversion vs. residence time for MMA polymerization.

Data and curve identification as in Figure 20.

removing all assumptions and using the full detailed model shown in Figure (dot-dash line) predicts the onset of instability at θ = 7 min.

The steady-state conversion vs. residence time for these three cases is shown in Figure 21. The simplified model overpredicts conversion for large residence times, which results from the choice of the small-r asymptote for the $\bar{i}$ relation, which from Figure 3 overpredicts $\bar{i}$ for large particles. At large residence times, the large particles make a significant contribution to the overall rate of monomer consumption. As long as the monomer droplets are present, however, the discrepancy in the steady-state solution does not affect the stability conclusions significantly.

Application of the stability criteria for the cases of the methylmethacrylate experimental studies noted in Table 1 shows complete agreement of the stability predictions between the detailed model and the case E simplified model. For the vinyl acetate experimental studies, there is complete agreement between the detailed model and the case C simplified model. The two levels of models agree at all experimentally reported operating conditions for these two monomers. Thus the simplified model analysis may be useful in providing a quick and easy method for studying the stability features of an operating region. The more cumbersome full model bifurcation analysis and numerical simulation studies can always be used to study regions of interest in greater detail. As discussed by Rawlings and Ray (1985, 1986b), one should also examine the amplitude of the oscillations in unstable regions. Even though the model predicts instability, the amplitude of the oscillation in monomer conversion can be so small that the experimental data would appear to be stable.

Chiang and Thompson (1979) analyzed a model similar to the simplified model of this work. The important difference between the models is as follows. Chiang and Thompson did not include the Heaviside function to stop particle initiation when the emulsifier concentration was below saturation. Their model was therefore linear at the outset and could not deal with transients that dipped below the critical micelle concentration (CMC). The current work started with a nonlinear model that was linearized about the steady state. The principal result of Chiang and Thompson's work is that the reactor is guaranteed to be stable if the steady-state particle area is less than one-half of the area of the soap in the feed. In the present notation this criterion is

$$m_s > \tfrac{1}{2} \tag{56}$$

From Eq. 39, this is equivalent to

$$\alpha < 1 \tag{57}$$

From Figure 7, one sees that Chiang and Thompson were describing region II, which is indeed stable for any choice of kinetic constant c.

Chiang and Thompson also developed a necessary and sufficient stability condition. There is a minor problem in comparing the current analysis to that of Chiang and Thompson. All of the results following Eq. 9 of their paper are only correct in the limit of vanishing initial particle size. Also, there is a sign error in the exponent in their Eq. A11. However, if we modify their analysis to account for these two problems, and transform their stability

criterion into our notation, it takes the form of Eq. 49. Unfortunately, Chiang and Thompson did not pursue their stability analysis beyond the criterion $\alpha < 1$ and thus were led to erroneous practical conclusions. In particular, their conclusion that $\alpha > 1$ leads to unstable operation and that this instability is independent of the value of c is totally incorrect.

Conclusions

A simple model for continuous emulsion polymerization reactors has been derived. The model retains the essential features for analysis of dynamics and stability and it provides great insight into the physical factors that control the stability of these reactors. An analytical solution to the model equations is developed that will be useful in simulation.

The most important conclusions from the present analysis are as follows:

1. The onset of oscillations in emulsion polymerization for steady-state operation above the CMC has nothing to do with the nonlinear on-off mechanism of particle nucleation at the CMC. The transition to instability arises for operation completely above the CMC. The presence of the CMC only controls the amplitude of the resulting oscillations.

2. The stability of the reactor depends on two key factors, as shown in Figure 8:

   (a) The slope w of the log $\bar{i}$ vs. log r (particle size) curve. For slopes $w \leq 1$, the reactor is stable for all operating conditions. For $w > 1$, the stability depends on

   (b) an operating factor α defined by Eq. 53. For values of $\alpha < 1$, the reactor is stable for all slopes w. However, when $w > 1$, the reactor is only stable for $\alpha < \alpha_c$ where α_c is given by Eq. 49. For any system, α varies as shown in Eq. 55 so that if $w > 1$, then high initiator concentration, lower surfactant concentration, and longer mean residence time lead toward instability.

3. One of the immediate consequences of 2a above is that reactors with Smith-Ewart case II kinetics (where $w = 0$) cannot oscillate under any operating conditions.

4. A second consequence of 2a above is that any kinetic mechanism or operating condition that causes the slope of the log $\bar{i}$ vs. log r curve to increase can increase the potential for instability and oscillatory operation. Examples of such mechanisms are radical desorption (through high chain transfer constants, addition of chain transfer agents, etc.), the presence of certain types of impurities, and the like.

5. At the transition to instability, relatively large-amplitude oscillations are seen immediately because at the bifurcation point (which is a center), the amplitude of the oscillation is determined only by the proximity of the steady state to the CMC.

It is interesting that these conclusions are in good agreement with trends observed from experimental reports of oscillatory behavior in emulsion polymerization reactors (Rawlings and Ray, 1986a). There is also good agreement between the detailed and simplified models at all experimentally reported operating conditions for methylmethacrylate and vinyl acetate polymerization.

Acknowledgment

The authors are grateful to the National Science Foundation, Union Carbide, and Hercules, Inc., and the sponsors of the University of Wisconsin Polymerization Reaction Engineering Laboratory for support of this research.

Notation

a = constant for $\bar{i}$, Eq. 12a
a_{em} = emulsifier coverage area on a micelle
a_{ep} = emulsifier coverage area on a particle
a_m = surface area of a micelle
b = constant for $\bar{i}$, Eq. 12b
c = kinetic model constant, Eq. 23a
$C_1 = 1 - d_m/d_p$
$C_2 = k_{po}\theta\, m_f V_{wf}$
$C_3 = d_m/M_{wt}M_f$
$C_4 = k_d\theta$
$C_5 = k_{mm}4\pi r_m^n N_a I_f \theta/V_{wf}$
$C_6 = k_{po}\theta/N_a V_m$
$C_7 = a_{em}S_f/a_m m_f$
$C_8 = a_{em}/a_{ep}V_{wf}$
$C_9 = k_{mm}4\pi r_m^n N_a m_f \theta$
$C_{10} = k_{mp}4\pi r_m^n N_a m_f \theta V_{wf}$
$C_{13} = k_{tro}D_m N_a V_m/k_{to}r_m^2 k_{po}$
$C_{14} = 4(4\pi r_m^n V_m I_f k_{mp}/k_{to})^{1/2}N_a$
$C_{18} = D_m M_{wt}/2r_m^2 k_{po}d_m$
d_m = monomer density
d_p = polymer density
D_m = effective diffusivity, $D_m = D_p D_w/(m_d D_p + D_w)$
D_p = diffusivity of radicals in polymer particles
D_w = diffusivity of radicals in aqueous phase
f = initiator efficiency factor
$F(t', t)$ = concentration of polymer particles at time t born at time t'
g_p = gel effect for propagation reaction, k_p/k_{po}
g_{po} = propagation gel effect at $\phi = \phi_{sat}$
g_t = gel effect for termination reaction, k_t/k_{to}
g_{to} = termination gel effect at $\phi = \phi_{sat}$
g_{tr} = gel effect for chain transfer reaction, k_{tr}/k_{tro}
g_{tro} = chain transfer gel effect at $\phi = \phi_{sat}$
H = Heaviside or unit step function
$\bar{i}$ = average number of radicals per particle
I = initiator concentration
$I_b(a)$ = modified Bessel function of the first kind
k_d = initiator decomposition rate constant
$k_f = C_5 R_f V_{wf}$, Table 2
k_i = constant in simplified model's $\bar{i}$ relation, Eq. 13, Table 2
$k_m = C_8 k_f k_r^2/V_{wf}$, Table 2
k_{mm} = mass transfer coefficient for radical entry into micelles
k_{mp} = mass transfer coefficient for radical entry into particles
k_p = propagation rate constant
k_{po} = propagation rate constant at 0 conversion
$k_r = [(3 - w)/3C_6 g_{po}\phi_{sat}/(1 - \phi_{sat})k_t]^{1/(3-w)}$, Table 2
k_t = termination rate constant
k_{to} = termination rate constant at 0 conversion
k_{tr} = effective chain transfer rate constant
k_{tro} = chain transfer rate constant at 0 conversion
$k_x = C_2 C_3 g_{po}\phi_{sat}k_f k_i k_r^w(3 - w)/3$, Table 2
K = stability constant, Eq. 55, Table 3
m = micelle concentration, $m = m'H(m')$
m' = available free soap for micelles
m_d = micelle concentration deviation from steady state
m_d = monomer partition coefficient (see D_m above)
M = total monomer concentration
M_{wt} = monomer molecular weight
n = radical entry model order: $n = 1$, diffusion model; $n = 2$, collision model
N_a = Avogadro's number
Q = volumetric flow rate
r = particle radius
r_m = radius of a micelle
R = aqueous phase free radical concentration
R_f = aqueous phase free radical concentration at feed conditions = $2fC_4/C_9$
s = Laplace transform variable
s_o = poles of Eq. 46
S = total emulsifier concentration
S_{wc} = critical micelle concentration
t = time
t' = time that a particle first appears in reactor
T = temperature

$\nu = (1/k_r)^{3-w}$, Table 2
V_m = volume of a micelle
V_R = total volume of contents of reactor
V_w = volume fraction of water in reactor
w = exponent of simplified model's $\bar{i}$ relation, Eq. 13, Table 2
x = overall monomer conversion

Greek letters

α = constant, Eq. 23b
α_c = value of α at transition to instability
γ = incomplete gamma function
Γ = complete gamma function
θ = reactor residence time
λ = largest eigenvalue of detailed model
π = pi
τ = particle age in residence times
T = period of sustained oscillation in residence times
ϕ = monomer volume fraction in particles
ϕ_{sat} = saturated monomer volume fraction in particles

Subscripts

f = feed conditions
s = steady state
d = deviation from steady state

Literature cited

Brooks, B. W., "Particle Nucleation Rates in Continuous Emulsion Polymerization Reactors," *Br. Polym. J.*, **5**, 199 (1973).

Brooks, B. W., H. W. Kropholler, and S. N. Purt, "Emulsion Polymerization of Styrene in a Continuous Stirred Reactor," *Polymer*, **19**, 193 (1978).

Chiang, A. S. T., and R. W. Thompson, "Stability of Continuous Emulsion Polymer Reactors," *J. Appl. Poly. Sci.*, **24**, 1935 (1979).

Churchill, R. V., *Operational Mathematics*, McGraw-Hill, New York (1972).

Cushing, J. M., *Integrodifferential Equations and Delay Models in Population Dynamics*, Springer-Verlag, Berlin (1977).

Davis, H. T., *Introduction to Nonlinear Differential and Integral Equations*, Dover, New York (1962).

Dickinson, R. F., "Dynamic Behaviour and Minimum Norm Control of Continuous Emulsion Polymerization Reactors," Ph.D. Thesis, Univ. Waterloo, Ontario (1976).

Gerrens, H., Kuchner, and G. Ley, "Zur Konzentrationsstabilität des Isothermen Reaktors," *Chemie.-Ing.-Techn.*, **43**, 693 (1971).

Gershberg, D. B., and J. E. Longfield, "Kinetics of Continuous Emulsion Polymerization," 54th AIChE Meet., New York (1961).

Gorber, D. M., "Dynamics of Continuous Emulsion Polymerization Reactors," Ph.D. Thesis, Univ. Waterloo, Ontario (1973).

Greene, R. K., R. A. Gonzales, and G. W. Poehlein, "Continuous Emulsion Polymerization—Steady State and Transient Experiments with Vinyl Acetate and Methyl Methacrylate," *Emulsion Polymerization*, I. Piirma, J. L. Gardon, eds., *Am. Chem. Soc. Symp. Ser.*, No. 24, Washington, DC, 341 (1976).

Hildebrand, F. B., *Advanced Calculus for Applications*, 2nd ed., Prentice-Hall, Englewood Cliffs, NJ (1976).

Jacobi, B., "Zur Kolloidchemie der Emulsionspolymerisation," *Angew. Chem.*, **64**, 539 (1952).

Jordan, D. W. and P. Smith, *Nonlinear Ordinary Differential Equations*, Oxford Univ. Press (1977).

Kiparissides, C., "Modelling and Experimental Studies of a Continuous Emulsion Polymerization Reactor," Ph.D. Thesis, McMaster Univ., Hamilton, Ontario (1978).

Kiparissides, C., J. F. MacGregor, and A. E. Hamielec, "Continuous Emulsion Polymerization. Modeling Oscillations in Vinyl Acetate Polymerization," *J. Appl. Poly. Sci.*, **23**, 401 (1979).

———, "Continuous Emulsion Polymerization of Vinyl Acetate. I, II, III," *Can. J. Chem. Engr.*, **58**, 48 (1980).

Kirillov, V. A., and W. H. Ray, "The Mathematical Modeling of Continuous Emulsion Polymerization Reactors," *Chem. Eng. Sci.*, **33**, 1499 (1978).

Ley, G., and H. Gerrens, "Mehrfache stationäre Zustände und periodische Teilchenbildung bei der Emulsionspolymerisation von Styrol im kontinuierlichen Rührkesselreaktor," *Makromol. Chem.*, **175**, 563 (1974).

Min, K. W., and W. H. Ray, "On the Mathematical Modeling of Emulsion Polymerization Reactors," *J. Macro. Sci. Revs.*, **C11**, 177 (1974).

Minorsky, N., *Introduction to Nonlinear Mechanics*, J. W. Edwards, Ann Arbor (1947).

Nomura, M., S. Sasaki, K. Fujita, M. Harada, and W. Eguchi, "Continuous Emulsion Polymerization of Vinyl Acetate," Am. Chem. Soc. Meet., San Francisco (1980).

Omi, S., T. Ueda, and H. Kubota, "Continuous Operation of Emulsion Polymerization of Styrene," *J. Chem. Eng. Japan*, **2**, 193 (1969).

O'Toole, J. T., "Kinetics of Emulsion Polymerization," *J. Appl. Poly. Sci.*, **9**, 1291 (1965).

Owen, J. J., C. T. Steele, P. T. Parker, and E. W. Carrier, "Continuous Preparation of Butadiene-Styrene Copolymer," *Ind. Eng. Chem.*, **39**, 110 (1947).

Penlidis, A., J. F. MacGregor, and A. E. Hamielec, "Dynamic Modeling of Emulsion Polymerization Reactors," *AIChE J.*, **31**, 881 (1985).

Rawlings, J. B., "Simulation and Stability of Continuous Emulsion Polymerization Reactors," Ph.D. Thesis, Univ. Wisconsin, Madison (1985).

Rawlings, J. B., and W. H. Ray, "The Structure of the Dynamic Behavior of Continuous Emulsion Polymerization Reactors," AIChE Ann. Meet., Los Angeles (1982).

———, "Bifurcation Structure and Stability of Emulsion Polymerization Reactors," AIChE Ann. Meet., Chicago (1985).

———, "The Modeling and Simulation of Continuous Emulsion Polymerization Reactors. I, II," *Polym. Engr. Sci.* (accepted 1986a).

———, "Stability of Continuous Emulsion Polymerization Reactors—A Detailed Model Analysis," *Chem. Eng. Sci.* (1986b).

Schork, F. J., "The Dynamics of Continuous Emulsion Polymerization Reactors," Ph.D. Thesis, Univ. Wisconsin, Madison (1981).

Schork, F. J., G. C. Chu, and W. H. Ray, "The Dynamics of Continuous Emulsion Polymerization Reactors," 73rd AIChE Meet., Chicago (1980).

Schork, F. J., and W. H. Ray, "On-Line Monitoring of Emulsion Polymerization Reactor Dynamics," *Emulsion Polymers and Emulsion Polymerization*, D. R. Bassett, A. E. Hamielec, eds., *Am. Chem. Soc. Symp. Ser.*, No. 165, Washington, DC, 505 (1981).

Scudo, F. M., "Vito Volterra and Theoretical Ecology," *Theor. Pop. Biol.* **2**, 1 (1971).

Smith, W. V., and R. H. Ewart, "Kinetics of Emulsion Polymerization," *J. Chem. Phys.*, **16**, 592 (1948).

Stakgold, I., *Green's Functions and Boundary Value Problems*, Wiley, New York, (1979).

Stockmayer, W. H., "Notes on the Kinetics of Emulsion Polymerization," *J. Poly. Sci.*, **24**, 314 (1957).

Yakovlev, A. Y., A. V. Zorin, and N. A. Isanin, "The Kinetic Analysis of Induced Cell Proliferations," *J. Theor. Biol.*, **64**, (1977).

Manuscript received Oct. 24, 1986, and revision received Mar. 5, 1987.